Proceeding of the 14th International Forum of Automotive Traffic Safety, 2017, pp 443-451
No.ATS.2017.504

Reliability-based design optimization of vehicle front-end shape for pedestrian-vehicle impact

Haiyang ZHANG[1], Xiaojiang LV [1,2], Dongdong TAN[2], Dayong ZHOU[1], Xianguang Gu[3]

[1] *Ningbo Geely Automobile Research and Development Co., Ltd., Zhejiang Key Laboratory of Automobile Safety Technology, Ningbo 315336, PR China*

[2] *State key Laboratory of Advanced Design and Manufacturing for Vehicle Body, Hunan University, Changsha, Hunan, 410082, PR China*

[3] *School of Mechanical and Automotive Engineering, Hefei University of Technology, Hefei, Anhui 230009, PR China*

Email: lvxiaojiang@geely.com

Abstract:

Background: To improve performance of vehicle pedestrian protection system, design optimization for vehicle front-end shape has proven rather essential and been extensively used. Nevertheless, an optimal design could become unacceptable when some uncertainties present. Furthermore, assessment of pedestrian injury values involves a number of criteria which may conflict with each other.

Objective: This paper is aimed to study the design optimization for vehicle front-end shape with considering the pedestrian-vehicle impact.

Method and Material: To address the issue, this paper presents the Reliability-Based Design Optimization (RBDO) of a vehicle front-end shape subjected to the pedestrian-vehicle impact cases. The multi-objective particle swarm optimization (MPSO) algorithm is implemented to generate the Pareto optimal set and the Monte Carlo Simulation (MCS) method is applied to perform the reliability analysis.

Results: It is show that the reliability of KBA is increased from 71.3% to 95.7% when the 90% reliability-based design is adopt and from 95.7% to 99.8% when the 99% reliability-based design is adopt. Compared with the results between the baseline and RBDO, the injury values of HIC and TBM are reduced to 50.8% and 8.8% relative to the initial design, respectively.

Conclusions: It was found that the result of reliability-based design was more conservative than the results of deterministic optimization as expected. As the variation of performance constraint functions raised by the uncertainties of design variables was considered, the reliability of the front-end shape design for the pedestrian protection was greatly improved in the real engineering application.

Keywords: Reliability-based design optimization, Vehicle front-end shape, Pedestrian protection, Multiobjective optimization

1 Introduction

With the increasing number of vehicle sales globally, traffic safety has become a major public health issue. Pedestrian are a significant proportion of road fatalities. Pedestrian deaths accounted for 22% of the traffic crash deaths worldwide and as high as 11% of those in USA, 20% of those in EU, 25% of those in China [1-2]. US data showed that approximately 80% of all pedestrian injuries were caused by the vehicle [3]. In the process of vehicle design, the safety performance of vehicle front-end design is key aspects controlling pedestrian injury severity [4-5].

As a complement to the experimental studies, mathematical models are widely used for vehicle-pedestrian impact.

In recent years, mathematical dynamic model (MADYMO) which is the most popular modelling tool for pedestrian kinematic predictions is frequently employed for vehicle safety design and pedestrian injuries evaluation [6-8]. Liu et al. used a pedestrian mathematical model in MADYMO to study the influences of vehicle impact speed, front shape and compliance properties on pedestrian dynamic responses [9]. Moreover, to investigate the effects of vehicle impact velocity and front-end structure on the dynamic responses of child pedestrians, an extensive parametric study was carried out using two child mathematical models at 6 and 15 years old [10]. Elliott et al. also used MADYMO pedestrian model to analyze the influences of vehicle speed, pedestrian speed and pedestrian gain on pedestrian post-impact kinematics [2].

Now, the optimization based on the CAE technology provides an effective and systematic way to seek an optimal design and its applications in vehicle safety design, have also been extensively explored [11]. For example, Kausalyah et al. optimized the geometry of the front-end structure based on the MADYMO utilizing the genetic algorithm method [12]. But that optimization problem cannot consider the uncertainty, which exists in material properties, geometries and manufacturing precision, etc. In order to take into account various uncertainty, Reliability-Based Design Optimization (RBDO) is introduced and aims at finding a reliable optimum solution by converting the deterministic constraints into probabilistic ones.

Nevertheless, vehicle front-end shape optimization for pedestrian-vehicle impact considering the uncertainty has received limited attention in the literature. Thinking for its significant practical value, this paper presents a comprehensive study approach of how different reliable optimization schemes are performed in the design of vehicle front-end shape under the pedestrian impact.

2 Theory and methodology

2.1 Reliability-based design optimization

A number of engineering designs often belong to Multi-objective Optimization Problem (MOP) in nature, as they often involve more than one criterion. To study the tradeoffs of these design objectives and explore available design options, the deterministic MOP can be formulated as:

$$\begin{cases} \min \quad f(x) = \left(f_1(x), f_1(x), \ldots\ldots, f_Q(x)\right)^T \\ s.t. \quad g_j(x) \le 0, \quad j = 1,2,\ldots\ldots,M \\ \qquad x^L \le x \le x^U \end{cases} \tag{1}$$

where $f(x)$ is a objective vector in the design space, $g_j(x)$ is the function representing the constraints, Q and M are the number of objectives and constraints, x^L and x^U are the lower and upper bounds of the vector of design variables x, respectively. Generally, the deterministic optimum designs without considering the uncertainty of design variables frequently push design constraints to the limit of boundaries.

The reliable design indicates an optimization subjecting to probabilistic bounds on the constraints as:

$$\begin{cases} \min \quad \mu\left(f_q(x)\right) \quad q = 1,2,\ldots\ldots,Q \\ s.t. \quad P\left(g_j(x) \le 0\right) \ge R_j, \quad j = 1,2,\ldots\ldots,M \\ \qquad x^L \le x \le x^U \end{cases} \tag{2}$$

Where μ is the vector of objectives mean and R_j is the desired reliability for satisfying functional constraint $g_j(x)$ ($g_j(x) > 0$ indicates failure). The reliable optimization design uses the probabilistic constraints to consider uncertainty of the design variables and parameters, which can stop pushing design constraints to the limit of boundaries [13-14].

2.2 Optimization approach

So as to meet the requirement of pedestrian protection, the RBDO is introduced to design the front-end shape for pedestrian-vehicle impact in multi-objective framework. This procedure shown in Figure 1 describes how to optimize the design parameters of the front-end shape for pedestrian-vehicle impact by minimizing pedestrian injuries. The Optimal Latin Hypercube Sampling (OLHS) technique adopted for constructing the surrogate models in the exploratory design space. The RBF models are constructed based on the response results of sampling points. The MPSO is applied to search the optimal solution set. The Monte Carlo Simulation (MCS) is applied to perform reliable analysis [15-17].

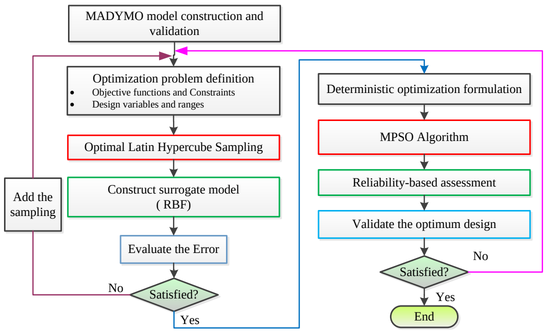

Figure 1. Flowchart of the reliability design optimization process

3 Simulation model and optimization problem definition

3.1 Simulation model

The MADYMO pedestrian model consists of 52 rigid bodies. The outer surface is described by 64 ellipsoids and 2 planes. For this paper, the standard 50th male adult is used, with an orientation perpendicular to the direction of vehicle travel. These models are extensively validated by TNO with cadaver tests for overall kinematics dynamic response for body segments and impact forces. The predicted impact responses of the models correlated reasonably well to the injury outcomes in accidents.

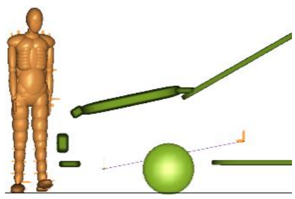

Figure 2.The baseline model of pedestrian-vehicle impact.

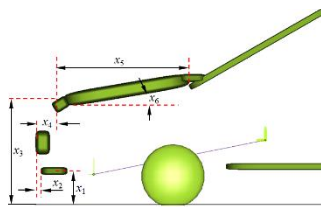

Figure 3. Design variables.

As shown in Figure 2, a baseline vehicle model is formulated according to the front-end shape of a main existing car. Vehicle front-end model consists of bumper, hood edge, hood top, windscreen, spoiler, cowl and wheels ellipsoids to approximate the exterior profile of a vehicle. The force-deformation property of vehicle front-end components is obtained according to Liu work [9-10]. A vehicle model made to impact with the right-side standing pedestrian at speed of 40 km/h. The braking deceleration of the vehicle model is simulated by frictional contact between wheels and the ground with a friction coefficient of 0.6 and the friction coefficient is 0.5 for the contacts between pedestrian and vehicle front structures. The injury risks of pedestrian are evaluated in terms of Table 1.

Table1. Tolerance levels of pedestrian injury parameters and baseline results

Injury parameters	Tolerance level	Baseline results
Head injury criteria (HIC)	1000	1301.5
Knee bending angle (KBA)	15 (°)	14.8 (°)
Tibia bending moment (TBM)	285 (Nm)	287.5 (Nm)
Femur bending moment (FBM)	430 (Nm)	278.1 (Nm)

3.2 Optimization problem definition

This study aims to optimize the front-end shape for reducing the pedestrian injury values. According to Table 1, the HIC and the TBM both exceed the performance limit. In order to meet the design requirements, improvements of the HIC and the TBM appear an effective way. From engineering experience, the front-end shape has important effect on pedestrian injury, thereby making the best possible combination of these components under pedestrian-vehicle impact conditions. Thus, these parameters are taken as design variables, as show in Figure 3. And description of design variables is shown in Table 2

Table 2. The description of design variables

Design variables	description
x_1 (mm)	Spoiler height, SH
x_2 (mm)	Horizontal distance between bumper and spoiler, DBS
x_3 (mm)	Bonnet leading edge height, BLEH
x_4 (mm)	Bumper lead, BL
x_5 (mm)	Hood horizontal length, HL
x_6 (°)	Hood angle, HA

Table 3. The value and probabilistic distribution of the design variables

Design variations	Distribution	COV(σ/μ)	Initial value	Boundary value	
				Lower	Upper
SH (x_1)	Normal	5%	280	240	340
DBS (x_2)	Normal	5%	-20	-60	40
BLEH (x_3)	Normal	5%	760	640	840
BL (x_4)	Normal	5%	120	0	150
HL (x_5)	Normal	5%	1000	700	1200
HA (x_6)	Normal	5%	12	8	18

Table 3 provides the list of the design variables, the values for the baseline design, as well as the corresponding lower and upper bounds. In order to take into account the uncertainties, the design variables are assumed to distribute normally in this study, whose coefficient of variation (cov(σ/μ)) is given as 5% from typical manufacturing and assembly tolerance. The values of design parameters with the function are defined by adjusting the change of coefficient relative to their initial values. The variations of design parameters are selected in terms of possible design changes allowed.

According to Table 1, the HIC and TBM could not meet the design requirements. For this reason, they are chosen as the design objectives. Considering that the design variables have an influence on other injuries, KBA and FBM are chosen as the constraints. Table 4 lists the responses of baseline design and the allowance of each constraint.

Table 4. The baseline and target design of the responses.

Responses	` Objectives		Constraints	
	HIC	TBM	KBA	FBM
	$f_1(x)$	$f_2(x)$	$g_1(x)$	$g_2(x)$
Baseline	1301.5	287.5	14.8 °	278.1 Nm
Target	Minimize	Minimize	≤15 °	≤430Nm

4 Optimization design

4.1. Deterministic optimization

The deterministic MOP of front-end shape for pedestrian-vehicle impact where no uncertainties are considered, is given by

$$\begin{cases} \min & f_1(x) \\ & f_2(x) \\ s.t. & g_1(x) \leq 15° \\ & g_2(x) \leq 430\,Nm \\ & x_i^L \leq x_i \leq x_i^U,\ \ x_i = (x_1, x_2, x_3, x_4, x_5, x_6)^T \end{cases} \tag{3}$$

For six continuous variables $X = (x_1, x_2, \ldots, x_6)$, the number of levels for each variable can be selected to be 6 and a total of 36 sampling points are generated in the design space by the OLHS method. Following this, the RBF models are constructed based on the response results of these sampling points. In this study, we adopt the MPSO Algorithm to optimize the front-end shape.

The optimal Pareto frontiers with the 100 iterations are obtained in Figure 4. It is noted that the Pareto frontier provides the designers with many applicable solutions. In fact, any point in the Pareto frontier can be a solution. For example, if the designer wishes to emphasize more on the HIC value, the TBM value must be compromised and become higher, and vice versa.

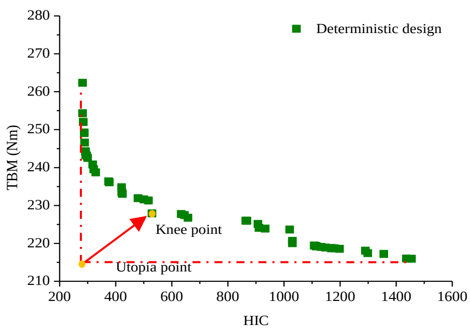

Figure 4. The Pareto front of deterministic optimization

In this study, The Minimum Distance Selection Method (TMDSM) is adopted for defining the most satisfactory solution from the Pareto-set [18]. The optimum results of two objectives and the two constraints of deterministic design are shown in Table 5. HIC and TBM injuries decrease 59.3% and 20.8% in deterministic optimization respectively. Based on the RBF surrogate model, a MCS using descriptive sampling points with given distribution is conducted for reliability assessment. When uncertainties introduced to the model, the reliability of two constraints are 71.3% for the KBA and 98.1% for the FBM respectively listed in Table 5.

Table 5. The results of the deterministic optimization design and initial design.

Description	Objectives		Constraints			
	$f_1(x)$	$f_2(x)$ /Nm	$g_1(x)$ / °		$g_2(x)$ /Nm	
	μ	μ	μ	R_j	μ	R_j
Initial	1301.5	287.5	14.8	–	278.1	–
Deterministic	529.5	227.8	14.9	71.3%	413.5	98.1%
Reduction%	59.3%	20.8%	-0.7%	–	-48.7%	–

Although the deterministic optimum designs obtain the lower injury of the head and lower extremity and meet the requirements of the design targets, there is more than 28% for the HIC chances to violate the design constraints in real world. To improve the reliability associated with these constraints, the reliability-based optimization is exercised for this problem.

4.2 Reliability-based design optimization

For the RBDO, the desired reliability of two design constraints (R_j) are set as 90% and 99%. And the minimize value of mean value is set for the two objectives, respectively. The reliability-based design is formulated as:

$$\begin{cases} \min & \mu(f_1(x)) \\ & \mu(f_2(x)) \\ s.t. & P(g_1(x) \le 15°) \ge R_j \\ & p(g_2(x) \le 430\,Nm) \ge R_j \\ & x_i^L \le x_i \le x_i^U,\ \ x_i = (x_1, x_2, x_3, x_4, x_5, x_6)^T \end{cases} \quad (4)$$

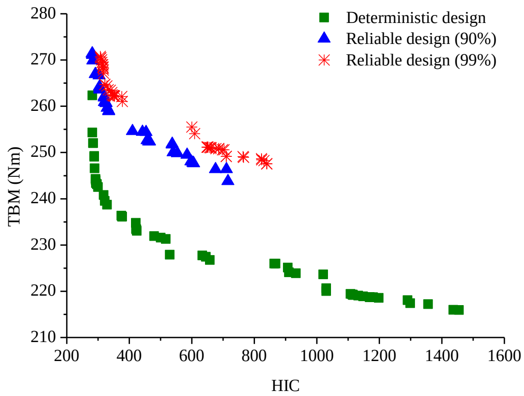

Figure 5. Pareto fronts for the multi-objective deterministic and reliable optimization designs.

The six design variables according to the probability distribution defined previously are incorporated, and RBDO is performed. The Pareto fronts are obtained using the MPSO algorithm. The MCS is consisted with 10,000 descriptive sampling points using given distribution in this study. Figure 5 presents the Pareto fronts for multi-objective deterministic and reliable designs.

In three Pareto fronts, each point represents one Pareto solution in different cases, which indicates the trade-off between HIC and TBM. Obviously, these two objectives strongly compete with each other: the lower HIC, the higher TBM. It is noted that the Pareto front of the 90% reliable design is farther away from the deterministic counterpart and the 99% reliable design is farthest away from the deterministic counterpart in Figure 5. The results of objective functions are listed in Table 6.

Table 6. Comparative of the optimization and initial results

Obj	Target	Initial	Deteriministic		90% Reliable		99% Reliable	
			Value	Effect	Value	Effect	Value	Effect
$f_1(x)$	Min.	1301.5	529.5	59.3%	540.6	58.5%	612.2	53.0%
$f_2(x)$	Min.	287.5	227.8	20.8%	250.0	13.0%	254.1	11.6%

Table 7. Constraint results of deterministic and reliability analysis

Description	Deterministic		90% Reliable		99% Reliable	
	Solution	R_j	μ	R_j	μ	R_j
$g_1(x)$	14.9	71.3%	9.1	95.7%	7.6	99.8%

$g_2(x)$	413.5	98.1%	374.0	100%	377.1	100%

From Table 6, with the enhancement of reliability value, the HIC and TBM are increased. As expected, the result from 90% and 99% reliable optimization is conservative compared to the one from deterministic optimization, which results from the fact that the uncertainties of the design variables is taken into account. It means that the 90% and 99% reliability of front-end shape design optimum goal is achieved when the worst-case tolerances of design variables are considered.

The reliability values shown in Table 7 are presented. As expected, the reliability value of KBA for the deterministic optimization is less than the desirables. It is noted that the reliability of KBA is increased from 71.3% to 95.7% when the 90% reliability-based design is adopt and from 95.7% to 99.8% when the 99% reliability-based design is adopt. The results also demonstrate that the KBA is more reliable using 99% reliability-based design. Thus, the 99% reliability-based design is chosen for engineering application.

4.3 Comparison and validation of optimization results

Figure 6 shows animation results of the baseline, deterministic and reliable optimization design at different times. Compared with Figure 6, the head impact point is obviously different at the baseline, deterministic and reliable optimization design schemes. Table 8 show design variable parameters of the different optimization designs.

Table 8. Design variable parameters of the different optimization designs

	x1	x2	x3	x4	x5	x6
Initial design	280	-20	760	120	1000	12
Deterministic design	306.2	23.1	700.5	59.2	1013.9	8.2
Reliable design (90%)	279.6	16.5	676.3	61.6	826.2	17.0
Reliable design (99%)	276.1	15.7	682.6	46.7	869.9	17.3

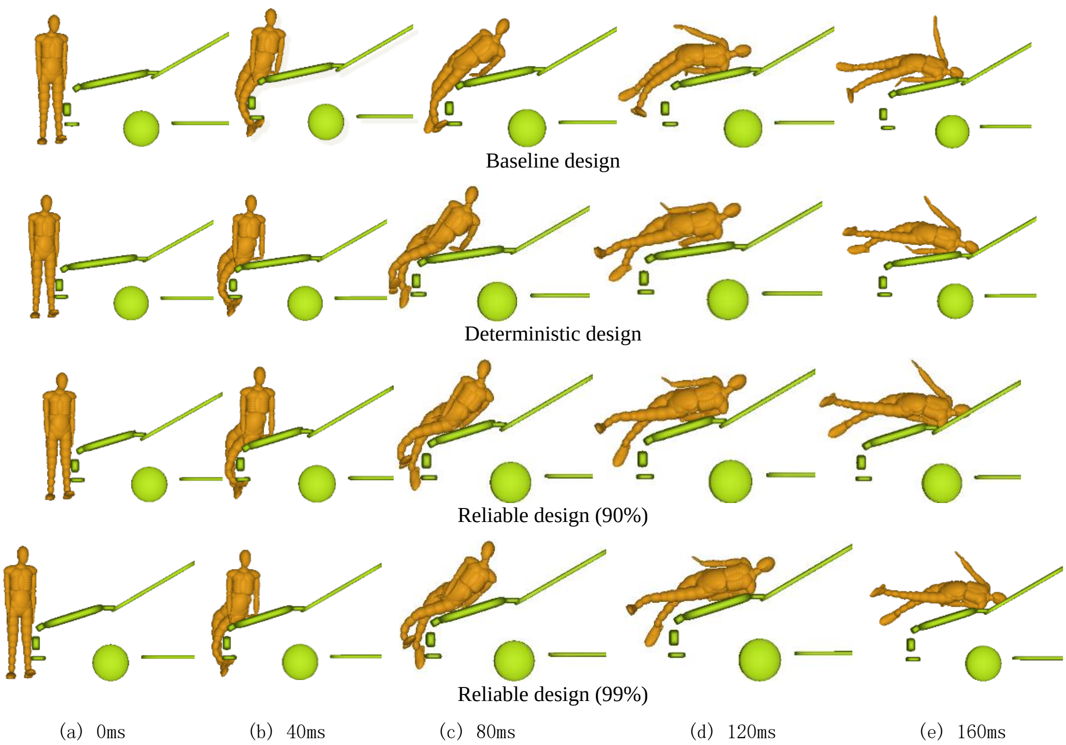

Figure 6. Animation after the baseline, deterministic and reliable optimization design.

According to the response values of simulation, the results between the baseline and optimal is compared in Table 9. The injury values of HIC and TBM are reduced to 50.8% and 8.8% relative to the initial design, respectively. Thus, the optimization result satisfies the design requirements. In summary, the presented method is effective for the front-end structure design, and these results show that the optimal design has improved the pedestrian safety significantly.

Table 9. The Comparison of the results between the baseline and optimal design.

Description		Baseline	Optimal result			Reduction (%)
			Knee point	Madymo Simulation	Error (%)	
Objectives	$f_1(x)$	1301.5	612.2	639.9	4.5	50.8
	$f_2(x)$	287.5	254.1	262.1	3.1	8.8
Constraints	$g_1(x)$	14.8	7.6	7.9	3.9	46.6
	$g_2(x)$	278.1	377.1	359.0	4.8	−29.1

5. Conclusions

A system approach has been developed to design and optimize the vehicle front-end shape in this study. The numerical model of pedestrian-vehicle impact was constructed. Then, the Optimal Latin Hypercube Sampling (OLHS) method was adopted for Design of Experiment (DOE) and the surrogate model was constructed through RBF. The optimal problems involving in a number of objectives were solved by the multi-objective particle swarm optimization (MPSO) algorithm in this study. In order to take into account the uncertainties of design variables, the Monte Carlo simulation (MCS) is used to reliability analysis. It was found that the result of reliability-based design was more conservative than the results of deterministic optimization as expected. As the variation of performance constraint functions raised by the uncertainties of design variables was considered, the reliability of the front-end shape design for the pedestrian protection was greatly improved in the real engineering application.

Acknowledgement

This work is supported jointly by Science Fund of State Key Laboratory of Advanced Design and Manufacturing for Vehicle Body (31525008) and the Open Fund of Zhejiang Key Laboratory of Automobile Safety Technology (No. 2009E10013).

References

[1] WHO, 2013. World health report 2013: Research for universal health coverage. World Health Organization.
[2] Elliott, J.R., Simms, C.K., Wood, D.P., 2012. Pedestrian head translation, rotation and impact velocity: The influence of vehicle speed, pedestrian speed and pedestrian gait. Accident Analysis and Prevention 45, 342-353.
[3] Zhang, G., Cao, L., Hu, J., Yang, K.H., 2008. A field data analysis of risk factors affecting the injury risks in vehicle-to-pedestrian crashes. Annu. Proc. Assoc. Adv. Automot. Med..
[4] LV Xiaojiang, WANG Chun, LIU Weiguo, et al. Optimization of front-end styling design for a passenger car based on pedestrian protection [J]. ***J Automotive Safety and Energy,*** 2011, **2**(3): 206-211. (in Chinese)
[5] LV Xiaojiang, LIU Weiguo, ZHOU Dayong, et al. Research of front-end styling design for a SUV based on pedestrian protection [J]. ***Automobile Tech,*** 2013(3): 37-41. (in Chinese)
[6] Guo, R., Yuan, Q., Sturgess, C., Hassan, A., Li, Y., Hu, Y., 2006. A study of an Asian anthropometric pedestrian in vehicle-pedestrian accidents using real-world accident data. International Journal of Crashworthiness 11 (6), 541-551.
[7] Yao, J., Yang, I., Otte, D., 2008. Investigation of head injuries by reconstructions of real-world vehicle-versus-adult-pedestrian accidents. Safety Science 46, 1103-1114.
[8] Simms, C.K., Wood, D., 2006a. Effects of pre-impact pedestrian position and motion on kinematics and injuries from vehicle and ground contact. International Journal of Crashworthiness 11 (4), 345-356.
[9] Liu, X.J., Yang, J.K., LO ̇VSUND, P., 2002. A study of influences of vehicle speed and front structure on pedestrian impact responses using mathematical models. Traffic Injury Prevention 3, 31-42.
[10] Liu, X.J., Yang, J.K., 2003. Effects of vehicle impact velocity and front-end structure on dynamic responses of child pedestrians. Traffic Injury Prevention 4, 337-344.
[11] Gu, X.G., Lu, J.W., 2014. Reliability-based robust assessment for multiobjective optimization design of improving occupant restraint system performance. Computers in Industry 65 (8), 1169-1180.
[12] Kausalyah, V., Shasthri, S., Abdullah, K.A., Idres, M.M., Shah, Q.H., Wong, S.V., 2014. Optimization of vehicle front-end geometry for adult

and pediatric pedestrian protection. International Journal of Crashworthiness 19 (2), 153-160.
[13] Zhang, Y., Sun, G.Y., Xu, X.P., Li, G.Y., Li, Q., 2014. Multiobjective crashworthiness optimization of hollow and conical tubes for multiple load cases. Thin-Walled Structures 82, 331-342.
[14] Gu, X.G., Lu, J.W., 2014. Reliability-based robust assessment for multiobjective optimization design of improving occupant restraint system performance. Comput Ind 65(8), 1169-1180.
[15] Gu, X.G., Sun, G.Y., Li, G.Y., Mao, L.C., Li, Q., 2013. A comparative study on multiobjective reliable and robust optimization for crashworthiness design of vehicle structure. Struct Multidisc Optim.
[16] LEE Y, JOO Y, PARK J, KIM Y, YIM H. Robust design optimization of frontal structures for minimizing injury risks of flex pedestrian legform impactor. International Journal of Automotive Technology 2014; 15(5): 757-764.
[17] Zhang, Y., Sun, G.Y., Xu, X.P., Li, G.Y., Li, Q., 2014. Multiobjective crashworthiness optimization of hollow and conical tubes for multiple load cases. Thin-Walled Structures 82, 331-342.
[18] Sun GY, Li GY, Hou SJ, Zhou SW, Li W, Li Q. Crashworthiness design for functionally graded foam-filled thin-walled structures. Materials Science and Engineering A 2010; 527(7-8):1911-1919.